Available online at www.sciencedirect.com
SCIENCE DIRECT®
Molecular and Cellular Probes 17 (2003) 5–10
MOLECULAR AND CELLULAR PROBES
www.elsevier.com/locate/ymcpr

Tissue-specific expression pattern of bovine prion gene: quantification using real-time RT-PCR

Ales Tichopad, Michael W. Pfaffl, Andrea Didier*

Institute of Physiology, FML Weihenstephan, Technical University of Munich, Weihenstephaner Berg 3, 85354 Freising, Germany

Received 8 May 2002; revised 4 November 2002

Abstract

In recent studies PrP mRNA was determined mostly by in situ hybridisation or Northern Blot analysis—methods not suitable for absolute quantification of mRNA copy numbers. Herein we report on bovine prion mRNA quantification using calibrated highly sensitive externally standardized real-time RT-PCR with LightCycler instrument. Total RNA was isolated from nine different regions of the CNS and seven peripheral organs. PrP^c mRNA copy numbers could be determined in all tissues under study. In approval with prior studies high mRNA level was found in Neocortex and Cerebellum. Lymphatic organs showed at least as high expression levels of prion mRNA as overall brain. Lowest expression was detected in kidney. Results of our study provide insight into the involvement of different organs in pathogenesis with respect to prion mRNA expression. LightCycler technology is currently considered the most precise method for nucleic acid quantification and showed to be powerful tool for further studies on prion diseases pathogenesis.

Keywords: Prion; Absolute quantification; Cattle; mRNA expression; Real-time RT-PCR

1. Introduction

Cellular prion protein (PrP^c) [1] a glycosylphosphatidyl inositol (GPI) anchored glycoprotein [2] expressed in numerous cell types [3] and tissues is suspected to be involved in the pathogenesis of prion diseases [4,5]. These neurodegenerative disorders are described in many species such as cattle (BSE), sheep (Scrapie), mink (TME), cats, (FSE) and also in humans (CJD) (for overview see 5). Alterations are histopathologically characterised by accumulation of pathogenic prion protein (PrP^{sc}) isoform. During disease progression PrP^c serves as a substrate molecule for PrP^{sc} that acts as a template [4–6]. Due to direct interaction between these two types of molecules PrP^c undergoes autocatalytic conformational changes and turns PrP^{sc}. Unlike PrP^c that has a more α-helical content, PrP^{sc} mainly shows β-sheeted structure [7,8]. As no other pathogens or nucleic acids seem to be involved in this process, it is called the 'protein-only hypothesis' [9].

Pathological alterations are mostly related to the central nervous system (CNS), but some early studies indicated that in pre-clinical stages of disease progression peripheral organs might play a crucial role [10–12] in pathogenesis. In this regard lymphoid organs are already of long-term high interest [13–14].

Expression of prion gene in neuronal and non-neuronal tissues has to be taken into special consideration for a better understanding of its role in organism as well as in prion disease pathogenesis and for consumption risk assessment. Spread of PrP^{sc} from peripheral organs to the CNS is poorly understood to date. Nevertheless it becomes more apparent, that cells of the immune system play an important role in PrP^{sc} accumulation and distribution [15,16]. Amount of PrP^c mRNA in these cells and subsequent translation product abundance probably play a role in disease initiation and progression. It is likely that cells with higher expression of PrP^c pose higher risk of conversion to and accumulation of PrP^{sc}.

Real-time RT-PCR using SYBR Green I technology [17] provides an excellent and highly sensitive method for absolute quantification of mRNA expression. Using an external calibration curve based on plasmid DNA the quantification model showed higher sensitivity, exhibited a larger quantification range, had a higher reproducibility, than models using recombinant RNA or diluted PCR product as calibration curve [18].

* Corresponding author. Tel.: +49-8161-713511; fax: +49-8161-714204
E-mail address: michael.pfaffl@wzw.tum.de (M. Pfaffl)

0890-8508/03/$ - see front matter © 2003 Elsevier Science Ltd. All rights reserved.
doi:10.1016/S0890-8508(02)00114-7

Getting insight into prion gene expression in tissues and organs possibly under various treatments is an essential starting point for further study of protein conversion and PrP^{sc} accumulation. Tissue-specific expression pattern determined with high reproducibility and accuracy is also essential for understanding poorly explained natural role of prions in organism. Herein we show results concerning prion mRNA expression in CNS and peripheral organs as well as we test suitability of above-mentioned method.

2. Material and methods

Three healthy male Holstein-Frisian calves at the age of six month and three healthy adult 'Brown Swiss' cows were selected for tissue material sampling. Animals were slaughtered using ordinary procedure according to EU's established hygienic policy at the Bayerisch Landesanstalt für Tierzucht, Grub. Following organs were sampled: Neocortex, Cerebellum, Thalamus, Hypothalamus, Pituitary gland, Medulla oblongata, Pars cervicalis, Pars thoracalis and Pars lumbalis, this all with respect to CNS. Concerning peripheral organs, samples of bronchial lymph nodes, spleen and thymus with respect to lymphoid organs together with muscle, liver, kidney and lung were gathered. For each region samples from minimally three animals were taken (see Table 1), immediately frozen in liquid nitrogen and then stored in -80 °C until RNA extraction procedure was performed.

Total RNA was extracted with commercially available preparation peqGOLD TriFast (Peqlab; Germany) utilizing single step modified liquid separation procedure [19]. Constant amounts of 1000 ng of RNA were reverse-transcribed to cDNA using 200 units of MMLV Reverse Transcriptase (Promega; USA) according to the manufacturers instructions. Fifteen randomly chosen control samples without reverse-transcriptase (RT-negative) were assayed as negative controls for RT reaction.

For usage as a standard the prion gene was cloned into pCR®4-TOPO® vector using TOPO TA Cloning® Kit for Sequencing (Invitrogen; The Netherlands). This circular construct was linearized with NotI restriction endonuclease (MBI Fermentas, Lithuania) and its purity was inspected on a 1% agarose gel. For standard curve acquisition five serial dilutions of double stranded plasmid DNA ranging from 10^3 to -10^7 molecules were then prepared (2×10^3 to 2×10^7 plasmid DNA molecules).

To verify PrP containing plasmid, it was sequenced by MWG Biotech (Germany) and showed 100% homology to the sequence in EMBL and GenBank accession number AF117327.

All measuring of nucleic acid concentrations were done at OD_{260} nm on spectrophotometer (BioPhotometer® Eppendorf; Germany) with 220 – 1600 nm UVettes®. PrP primers flanking a 262 bp fragment were constructed as follows: Forward 5: AAC CAA GTG TAC TAC AGG CCA, Reverse 5: AAG AGA TGA GGA GGA TCA CAG. Conditions for PCR were optimized in a gradient cycler (Mastercycler Gradient; Eppendorf; Germany) and subsequently in LightCycler analyzing melting curve of product acquired. This was done with respect to primer annealing temperature, primer concentration, template concentration and number of cycles applied.

Real-time PCR using SYBR Green I technology [18] in LightCycler with the above-mentioned primers was carried out amplifying cDNA of biological sample, negative controls and five plasmid DNA standards. Master-mix was prepared as follows: 6.4 μl of water, 1.2 μl $MgCl_2$

Table 1
Parameters of quantification. n, number of samples. Where n = 3, only calf samples were available due to different slaughtering procedure; y(RNA), yield of RNA in 1 mg of tissue; CV, coefficient of variation; copy/RNA, number of PrP mRNA copies in 1 ng of total RNA; copy/tissue, number of PrP mRNA copies in 1 mg of tissue

Tissue	n	y(RNA) (ng)	CV%	Copy/RNA (molecules)	CV%	Copy/tissue (molecules)	CV%
Neocortex	6	617	10.9	66154	50.9	4.1×10^7	50.3
Cerebelum	6	735	22.9	40095	12.5	3.0×10^7	30.1
Thalamus	6	445	15.4	9408	50.9	4.2×10^6	51.5
Hypothalamus	6	388	29.3	5621	43.3	2.2×10^6	63.4
Pituitary gland	3	311	17.3	6379	68.2	2.0×10^6	74.1
Medulla oblong	3	336	15.5	17026	5.6	5.7×10^6	20.8
Pars cervicalis	3	298	17.3	20483	45.9	6.1×10^6	33.7
Pars thoracalis	3	388	51.7	12039	60.5	4.7×10^6	64.7
Pars lumbalis	3	308	43.2	11008	59.5	3.4×10^6	90.9
Spleen	3	2600	16.5	5911	8.8	1.5×10^7	24.6
Lymph nodes	3	3150	16.8	21360	16.9	6.7×10^7	25.9
Thymus	3	2580	41.4	4320	25.9	1.1×10^7	18.2
Muscle	6	352	31.3	5649	117.8	2.0×10^6	81.3
Liver	6	2990	14.5	3316	87.7	9.9×10^6	76.6
Kidney	6	1200	50.1	138	41.6	1.7×10^5	49.6
Lung	6	1320	30.7	1222	29.3	1.6×10^6	56

(25 mM), 0.2 μl of each primer (20 pmol), 1.0 μl Fast Start DNA Master SYBR Green I (Roche Diagnostics; Switzerland) mix. Nine μl of mastermix and 25 ng of reverse transcribed total RNA or plasmid DNA of the respective concentration. Following amplification program was applied: after 10 min of denaturation at 95 °C 40 cycles of 4-segment amplification were accomplished with: 15 s at 95 °C for denaturation, 10 s at 62 °C for annealing, 20 s at 72 °C for elongation and 5 s at 83 °C appended for a single fluorescence measurement above melting temperature of possible primer-dimers. This fourth segment eliminates a non-specific fluorescence signal and ensures accurate quantification of desired product. Subsequently, a melting step was performed consisting of 10 s at 95 °C, 10 s at 60 °C and slow heating with a rate of 0.1 °C per second up to 99 °C with continuous fluorescence measurement.

Quantification of PrP gene expression was performed in terms of PrP cDNA copies using LightCycler software 3.5 based on 'Second Derivative Maximum Method' (Roche Diagnostics; Switzerland). In this method a second derivative maximum within exponential phase of amplification curve is linearly related to a starting concentration of template cDNA molecules.

The mean, standard deviation (SD) and coefficient of variance (CV) was then calculated from obtained numbers of copies re-counted per 1 ng of total RNA and 1 mg of tissue for every organ and region over all six animals. Expression per mg of tissue was obtained as follows:

$$n_{tissue} = y(RNA) \times n_{cDNA}$$

where n_{tissue} is number of PrP^c mRNA copies in 1 mg of tissue, y(RNA) is for the yield of total RNA from 1 mg of tissue and n_{cDNA} means number of PrP cDNA copies in 1 ng of total cDNA. The distribution of all data sets was tested (Kolmogorov-Smirnov normality test) and, where necessary, data were normalized using common logarithm. Eventually one-way analysis of variance and t-tests were applied (SigmaStat; Jandel Scientific Software SPSS). Tissue-specific contrasts were inspected employing Tukey Test (SigmaStat; Jandel Scientific Software SPSS).

3. Results

Sensitivity of the LightCycler RT-PCR was evaluated using different starting amounts of mRNA and standard curve. SYBR Green I fluorescence determination at the elevated temperature 83 °C resulted in a reliable and sensitive cDNA quantification assay with high linearity (Pearson correlation coefficient = 0.99) over five orders of magnitude from 2×10^3 to 2×10^7 recombinant standard DNA start molecules (Fig. 1).

To verify real-time RT-PCR products derived either from plasmid or tissue total RNA a melting curve analysis on LightCycler (Roche) and gel electrophoresis were performed. Products showed no primer dimers, single sharp peak, identical melting points and expected length of 262 bp in gel electrophoresis.

Real-time PCR efficiencies were calculated from the given slopes (three repeats) in LightCycler Software 3.5

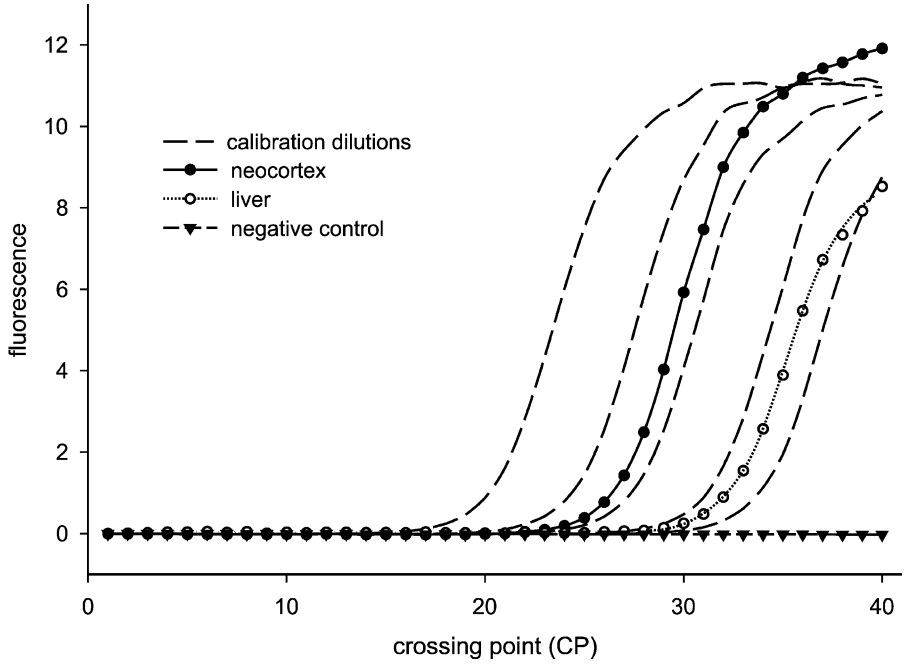

Fig. 1. Example of real-time PCR amplification curves obtained by plotting fluorescence data against their cycle number. Five calibration dilutions (2×10^7–2×10^3 copies) are shown together with two biological sample of Neocortex (4.25×10^5 copies) and liver (7.41×10^3 copies) and a negative control (without nucleic acid input).

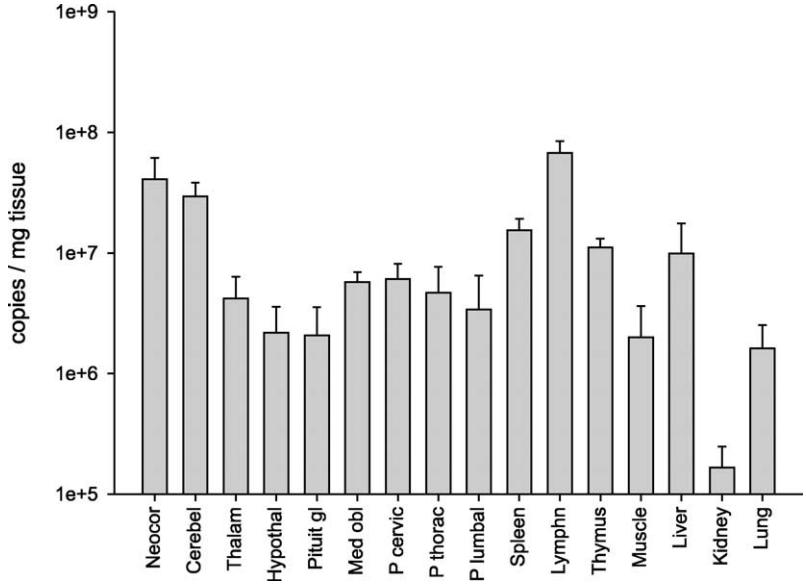

Fig. 2. Quantification of PrP mRNA copies in 1 mg of tissue. Error lines indicate SD.

(Roche) and showed efficiency rates per cycle in the DNA calibration curve model of $E = 1.90$. Sensitivity, linearity and reproducibility of the developed PrP real-time PCR assay allows for the absolute and accurate quantification of cDNA molecules even in tissues with low abundances down to a few molecules. After optimization of RNA extraction procedure no contamination by DNA was detectable in RT-negative samples.

Significantly ($p < 0.01$; log transformed) different amounts of total RNA were obtained ranging from 308 ng/mg (Pars lumbalis) to 3150 ng/mg of tissue (lymph nodes). For overview see Table 1. Inter-assay variation, between different real-time PCR runs, with the same cDNA ($n = 6$) was $<10\%$. Intra-assay variation, within one real-time PCR run, was $<5\%$. Inter-assay variation with the same total RNA but reverse-transcribed in different reactions had variance ranging from 7.2 to 30%.

No significant difference (t test, $p = 0.05$) in PrP RNA expression was found between both groups of animals concerning mean overall values and with respect to individual organs. For the purpose of statistical analysis the group of six animals was considered homogenous.

Significantly ($p < 0.01$; log transformed) different numbers of prion mRNA copies were determined in 1 ng of total RNA. The results of quantification are shown in Table 1. The highest PrP mRNA amount per 1 ng of total RNA was found in Neocortex. The lowest was found in kidney. As for the neuronal tissues, second highest levels of mRNA expression was found in Cerebellum. Lymph nodes showed highest content of PrP mRNA in 1 ng of total RNA within the three lymphoid organs studied. From other organs the highest copy number of PrP mRNA was determined in liver.

Re-counted to 1 mg of tissue, the highest expression level was found in lymph nodes and the lowest in kidney (Table 1, Fig. 2). Neocortex showed the highest expression within all CNS. Other neuronal tissues including different parts of spinal cord express similar levels of PrP. For tissue-specific contrast see Table 2.

4. Discussion and conclusions

Intuitive accord of our results with previously published data shows that real-time RT-PCR using LightCycler is reliable and powerful instrument to study pathogenesis of prion disease on mRNA level. Nevertheless, it makes these studies comparable and reproducible. It yields valued outputs as to levels of prion mRNA

Table 2
Tissue-specific contrasts in PrP mRNA copy number in 1 mg of tissue. The sign ‘ + ’ indicates significant ($p < 0.05$) difference, ‘ − ’ vice versa

p<0.05	Lymph n	Neocor	Cerebel	Spleen	Thymus	Liver	P cervic	Med obl	P thorac	Thalam	P lumbal	Hypothal	Pituit gl	Muscle	Lung	Kidney
Lymph n		-	-	-	-	+	+	+	+	+	+	+	+	+	+	+
Neocor	-		-	-	-	+	+	+	+	+	+	+	+	+	+	+
Cerebel	-	-		-	-	-	-	-	+	+	+	+	+	+	+	+
Spleen	-	-	-		-	-	-	-	-	-	-	+	+	+	+	+
Thymus	-	-	-	-		-	-	-	-	-	-	-	-	+	+	+
Liver	+	+	-	-	-		-	-	-	-	-	-	-	-	-	+
P cervic	+	+	-	-	-	-		-	-	-	-	-	-	-	-	+
Med obl	+	+	-	-	-	-	-		-	-	-	-	-	-	-	+
P thorac	+	+	+	-	-	-	-	-		-	-	-	-	-	-	+
Thalam	+	+	+	-	-	-	-	-	-		-	-	-	-	-	+
P lumbal	+	+	+	-	-	-	-	-	-	-		-	-	-	-	+
Hypothal	+	+	+	+	-	-	-	-	-	-	-		-	-	-	+
Pituit gl	+	+	+	+	-	-	-	-	-	-	-	-		-	-	+
Muscle	+	+	+	+	+	-	-	-	-	-	-	-	-		-	+
Lung	+	+	+	+	+	-	-	-	-	-	-	-	-	-		+
Kidney	+	+	+	+	+	+	+	+	+	+	+	+	+	+	+	

in different tissues. The reverse transcription reaction is the most significant cause of error. From our and other's experiences. We consider its efficiency between 30–70%, depending on sample type. Apparently, there is a general tissue-specific effect on quantification results. The RNA extraction procedure is also an important factor influencing quantification accuracy, if the copy number is expressed per tissue weight. This becomes clear after comparison of variance in PrP mRNA amounts in total extracted RNA and in tissue (Table 1). Concerning different RNA copy numbers per ng total RNA and per mg tissue, discussion has to face two different interpretations. Firstly, copy numbers per ng total RNA give good insight into total PrP^{c} expression potential of different organs. These data are more important for understanding of an early pathogenesis in prion disease. Secondly, the pattern of expression per tissue weight should have higher impact on consumption risk assessment of different organs. As mentioned in the introduction part, it is likely that organs with higher expression of PrP^{c} pose higher risk for conversion to and accumulation of PrP^{sc}. As daily food intake will be on gram level, PrP^{c} expression per mg tissue is important for consumer risk appraisal.

All three lymphatic organs express highly PrP mRNA, but fact that high total RNA yield was obtained from these tissues must be considered. This could possibly affect the re-calculation of copy number per weight of tissue. Nevertheless, our findings are consistent with role of PrP^{c} within immune system as suggested by Cashman [16] and with close prion-immune system linkage in general [15]. Nevertheless, they are in contrast to the earlier work of Robakis [20] where PrP was undetectable in normal rodent spleen. It is therefore necessary to focus more in detail on absolute PrP mRNA quantification in the above-mentioned organs and cells.

High PrP expression in neuronal tissues is consistent with works of Harris et al. [21,22] who were able to detect chicken prion protein mRNA in brain and a variety of organs by the means of in situ hybridisation and Northern Blot. But it has to be mentioned that above cited methods are semi-quantitative and under the detection abilities of real-time RT-PCR. Furthermore, they are not suitable for absolute quantification of PrP mRNA transcripts. Higher levels of expression in Neocortex and Cerebellum are coherent with several well-postulated hypothesis on PrP^{c} distribution in vertebrate organism and its ultimate role for normal neuronal function in CNS [23,24]. No apparent contrast in PrP mRNA levels was observed between white and gray matter of Neocortex, Medulla oblongata and Medulla spinalis (data not shown), although possible contamination during region segregation must be taken into account. In contrast, other regions of the brain as well as spinal cord showed no significant difference to other peripheral organs such as liver, muscle or lung. Kidney with its lowest expression was significantly different from all other tissues. Cells possibly responsible for higher expression levels in liver compared to muscle could be Kupffer's cells belonging to the antigen presenting subpopulation of white blood cells. Muscle and liver had different expression levels with more pronounced mRNA amount in the liver, which should have impact on consumption risk assessment. This gives a good intuitive sense, concerning that no PrP^{sc} infectivity has ever been detected within muscle tissue. We detected considerably low mRNA amounts in kidney compared to all above tissues. As we detected PrP mRNA in all tissues under study, it is probable that a post-transcriptional regulation finally determines PrP^{c} amount on protein level and its anchorage on the cell surface.

Acknowledgements

We thank the Bayerische Landesanstalt für Tierzucht at Grub for excellent technical support during the slaughtering and tissue sampling process.

References

[1] Prusiner SB. Novel proteinaceous infectious particles cause scrapie. Science 1982;216:136–44.
[2] Stahl N, Borchelt DR, Hsaio K, Prusiner SB. Scrapie prion protein contains a phosphatidylinositol glycolipid. Cell 1987;51:229–40.
[3] Brown HR, Goller NL, Rudelli RD, et al. The mRNA encoding the scrapie agent protein is present in a variety of non-neuronal cells. Acta Neuropathol 1990;80:1–6.
[4] Prusiner SB. Prions. Proc Natl Acad Sci USA 1998;95:13363–83.
[5] Liemann S, Glockshuber R. Transmissible spongiform encephalopathies. Biochem Biophys Res Commun 1998;250:187–90.
[6] Brandner S, Isenmann S, Raeber A, et al. Normal host prion protein necessary for scrapie-induced neurotoxicity. Nature 1996;379:339–43.
[7] Pan KM, Baldwin M, Nguyen J, et al. Conversion of alpha-helices into beta-sheets features in the formation of the scrapie prion proteins. Proc Natl Acad Sci USA 1993;90:10962–6.
[8] Safar J, Roller PR, Gajdusek DC, Gibbs CJ. Conformational transitions, dissociation, and unfolding of scrapie amyloid (prion) protein. J Biol Chem 1993;268:20276–84.
[9] Griffith JS. Self-replication and scrapie. Nature 1967;215:1043–4.
[10] Kimberlin RH, Walker CA. Pathogenesis of mouse scrapie: dynamics of agent replication in spleen, spinal cord and brain after infection by different routes. J Comp Pathol 1979;89:551–62.
[11] Kimberlin RH, Walker CA. Pathogenesis of scrapie (strain 263K) in hamsters infected intracerebrally, intraperitoneally or intraocularly. J Comp Pathol 1986;67:255–63.
[12] Kimberlin RH, Walker CA. Incubation periods in six models of intraperitoneally injected scrapie depend mainly on the dynamics of agent replication within the nervous system and not the lymphoreticular system. J Gen Virol 1988;69:2953–60.
[13] Fraser H, Dickinson AG. Pathogenesis of scrapie in the mouse: the role of the spleen. Nature 1970;226:462–3.
[14] Fraser H, Dickinson AG. Studies of the lymphoreticular system in the pathogenesis of scrapie: the role of spleen and thymus. J Comp Pathol 1978;88:563–73.
[15] Aucouturier P, Carp RI, Carnaud C, Wisniewski T. Prion diseases and the immune system. Clin Immunol 2000;96:79–85.

[16] Cashman NR, Loertscher R, Nalbantoglu J, et al. Cellular isoform of the scrapie agent protein participates in lymphocyte activation. Cell 1990;61:185–92.
[17] Morrison T, Weis JJ, Wittwer CT. Quantification of low-copy transcripts by continuous SYBR Green I monitoring during amplification. BioTechniques 1998;24:954–62.
[18] Pfaffl MW, Hageleit M. Validities of mRNA quantification using recombinant RNA and recombinant DNA external calibration curves in real-time RT-PCR. Biotechnol Lett 2001;23:275–82.
[19] Chomczynski P. A reagent for the single-step simultaneous isolation of RNA, DNA and proteins from cell and tissue samples. BioTechniques 1993;15:532–7.
[20] Robakis NK, Sawh PR, Wolfe GC, Rubenstein R, Carp RI, Innis MA. Isolation of a cDNA clone encoding the leader peptide of prion protein and expression of the homologous gene in various tissues. Proc Natl Acad Sci USA 1986;83:6377–81.
[21] Harris DA, Lele P, Snider WD. Localization of the mRNA for a chicken prion protein by in situ hybridization. Proc Natl Acad Sci USA 1993;90:4309–13.
[22] Harris DA, Falls DL, Johnson FA, Fischbach GD. A prion-like protein from chicken brain copurifies with an acetylcholine receptor-inducing activity. Proc Natl Acad Sci USA 1991;88:7664–8.
[23] Collinge J, Whittington MA, Sidle KC, et al. Prion protein is necessary for normal synaptic function. Nature 1994;370:295–7.
[24] Sakaguchi S, Katamine S, Nishids N, et al. Loss of cerebellar Purkinje cells in aged mice homozygous for a disrupted PrP gene. Nature 1986; 380:528–31.